Hindawi
Advances in Condensed Matter Physics
Volume 2018, Article ID 4847036, 8 pages
https://doi.org/10.1155/2018/4847036

Research Article

The Effect of Geometrical Parameters on Resonance Characteristics of Acoustic Metamaterials with Negative Effective Modulus

Xiao-Le Yan,[1] Li-Mei Hao,[1] Mei-Ling Men,[1] and Zhi Chen[2]

[1]*Department of Applied Physics, Xi'an University of Science and Technology, Xi'an 710054, China*
[2]*Department of Applied Physics, Northwestern Polytechnical University, Xi'an 710129, China*

Correspondence should be addressed to Li-Mei Hao; haolm@xust.edu.cn and Zhi Chen; c2002z@nwpu.edu.cn

Received 24 November 2017; Revised 7 February 2018; Accepted 28 February 2018; Published 4 April 2018

Academic Editor: Liyuan Zhang

There has been an explosion of interest in acoustic metamaterial in the last ten years. The tunable negative acoustic metamaterial is an important issue for designing metamaterials. The acoustic metamaterial is restricted by the narrow bandgap of sound waves for the local resonance of metamaterial unit cells. By shifting the sizes of the unit cell, the acoustic metamaterial could potentially overcome the limit of the narrow resonance frequency. In this research, we focus on the resonant behavior of split hollow sphere (SHS) in the waveguide. Firstly, we analyze the resonance characteristics of SHS and get an analytical formula for the effect of geometrical parameters on the resonance frequency. Furthermore, the resonance frequency of SHS is verified with finite-element method analysis based on COMSOL Multiphysics simulation. The results are in good agreement with theory model. It is observed that there is a blue shift of the resonance frequency with the gradual increase of the neck radius of SHS, a V-type response curve with the increase of inner radius of SHS, and a red shift with the increase of outer radius of SHS. Using the method of estimate of resonance, we could get a precisely controllable unit structure with negative effective modulus and offer a way to optimize the realization of double negative acoustic metamaterial.

1. Introduction

Acoustic metamaterial is a kind of man-made material that exhibit superior properties, and it is applied to control the direction of sound wave. The idea of negative effective density of acoustic metamaterial using local resonance unit was first proposed by Liu et al. in 2000 [1]. In this way, more researchers pay attention to local resonant acoustic metamaterial with negative effective density mass [2–10]. At the year of 2006, Fang et al. [11] designed a one-dimensional array consisted of split hollow cavity with subwavelength which is a new class of acoustic metamaterial with negative effective modulus at the ultrasonic frequency. Later on, Lee et al. [12] made a kind of one-dimensional acoustic metamaterial with splitting hollow on the side of hollow tube and confirmed that the acoustic metamaterial has the property of negative effective modulus at the frequency range of 0~450 Hz. A simpler version of two-dimensional negative effective modulus based on SHS was prepared by Ding et al. [13]. By 2015, Jing et al. [14] proposed a new kind of monopole resonance characteristics of balloon soft resonator to realize negative effective modulus. However, the main disadvantage of the local resonant acoustic metamaterials is that the response frequencies of different units are different and the frequency bands are narrow. Therefore, similar to electromagnetic metamaterials, the tunable negative acoustic metamaterial is an important issue in the acoustic research. The tunable range of resonant frequency is one of the important parameters in the application of acoustic metamaterials.

At present, active and passive methods have been adopted to control the resonance frequency of metamaterials with negative modulus [15–17]. Akl and Baz [15] controlled the Helmholtz resonator with negative modulus with by coupling with piezoelectric film and applying the electric field. There are many factors that influence the resonance characteristics of acoustic metamaterial unit, such as the shape, size,

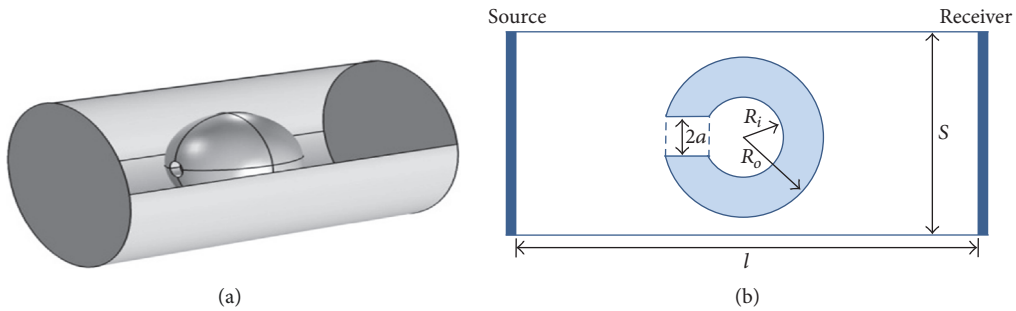

Figure 1: (a) The 3D scheme of the metamaterial unit cell. (b) The cross section of the cell.

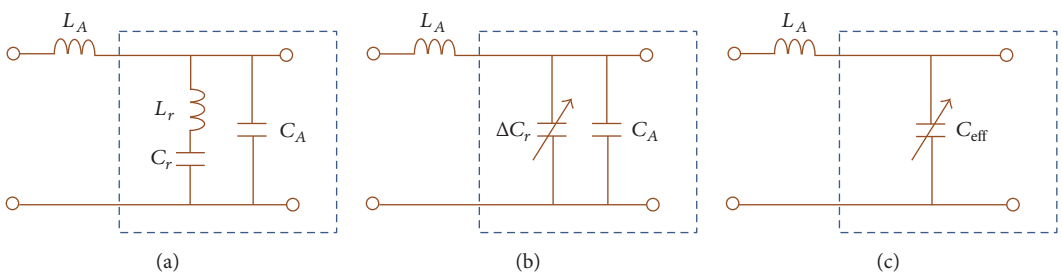

Figure 2: (a) An acoustic equivalent circuit using the impedance analogy. (b) The effective impedance circuit of SHS. (c) The effective impedance circuit of the two capacitors.

medium, and number of holes. Ding et al. [18] controlled the resonance frequency with negative modulus by shifting the hole size of SHS. Hao et al. [19] tuned the resonant frequency by changing the medium type of SHS. In addition, the resonant frequency can be controlled by multiple holes on the SHS [20]. At present, little attention has been paid to the precise relationship between the size of structure units and resonance frequency.

In this work, based on the Helmholtz theory and transmission line theory, the resonance characteristic of SHS was discussed. The effective bulk modulus and the amendment formula of resonance frequency were established. Furthermore, COMSOL Multiphysics with the finite-element method was used to design and simulate 3D structure of the acoustic metamaterials unit cell and to verify the effects of geometrical parameters on resonance characteristics consisting of size parameters of the neck radius, inner radius, and outer radius. This provides the basis and guidance for the design and fabrication of double negative acoustic metamaterials in arbitrary frequency by coupling structure units with negative mass density in the next step.

2. The Resonance Characteristics of SHS

2.1. Resonant Metamaterial Unit Cell. The Helmholtz resonators in [11] are arranged orthogonal to the propagation direction of the sound in the waveguide and the structure is successfully achieved negative effective bulk modulus. From transmission line concept, the equivalent circuit of a Helmholtz resonator is given by an LC circuit with no dissipation. And there is another LC section of the waveguide which is connected in parallel with the LC circuit. Based on this idea, we place a SHS in the middle of the cylindrical waveguide in the proposed metamaterial unit cell, as shown in Figure 1(a). The SHS is a type of Helmholtz resonator, including the sphere cavity and the short-tube formed by split hole, also called the neck. Here, it will be shown that the structure can be also used to support negative effective bulk modulus of acoustic metamaterial.

In Figure 1(b) a cross section of the metamaterial unit cell is shown. The cylindrical waveguide is driven at left end by a sound source and is measured at right end by a receiver. The cross section area of the waveguide is S, and the length is l. The SHS (a spherical cavity with the inner radius R_i and the outer one R_o, and a narrow neck with the radius a) is positioned at the source and levitated in the middle of the waveguide.

The equivalent circuit of the unit cell with lossless is given by an analogy circuit as Figure 2(a). In this model, the impedance of the waveguide is represented by the acoustic inertance L_A given by [21]

$$L_A = \frac{\rho l}{S} \tag{1}$$

and the acoustic compliance C_A, which is given by

$$C_{\mathrm{A}} = \frac{V}{\rho v_s^2}, \tag{2}$$

where ρ is the density of air, v_s is the sound velocity, and V is the volume of the air in the waveguide except the SHS. Additionally, the SHS can be modeled with acoustic inertance

$$L_r = \frac{\rho L_p}{S_p} \tag{3}$$

and acoustic compliance

$$C_r = \frac{V_p}{\rho v_s^2}, \tag{4}$$

where L_p is the effective length of the neck, S_p is the cross-sectional area of the one, and V_p is the effective volume of cavity.

2.2. The Effective Bulk Modulus of the Unit Cell. It is well known that, according to the dynamical theory, the vibration system is characterized by its mechanical impedance. Similarly, acoustic impedance Z_a describes the relationship between the sound pressure and the particle velocity, which is given by

$$Z_a = R_a + jX_a, \tag{5}$$

where R_a is the acoustic resistance and X_a is the acoustic reactance. The acoustic resistance represents the energy losses and the acoustic reactance is a concentrated expression of the inertia and elasticity of the system.

Since the fluid medium is air in the waveguide, the shear viscosity and thermal conductivity of the gas are too small enough and can be neglected. Therefore, the acoustic resistance is equal to zero in the analog circuit.

In the case of the acoustic metamaterial unit cell, if the waveguide acts as a simple low-pass filter (LPF), the SHS can be viewed as an "internal heat" as shown in Figure 2(a). The resonance frequency of the SHS falls within the passband of the LPF. In the cylindrical waveguide, there is just one propagating acoustic mode below some cut-off frequency.

In order to simplify the question, the equivalent parameters method is used to the analysis of acoustic reactance. We use the effective acoustic compliance ΔC_r representing the quantity of the inertia and elasticity of SHS which is connected in parallel with C_A as shown in Figure 2(b). Consequently, the parallel combination of the two capacitors has one all effective acoustic compliance C_{eff}, Figure 2(c). C_{eff} could vary in a large number for local resonance and plays a major role in the circuit.

In the context of acoustics, the bulk modulus of unit cell B_A is an important parameter of sound propagation [11]. Suppose that sound propagation is an isentropic process, for which $v_s^2 = \partial p/\partial\rho = B_A/\rho$; bulk modulus $B_A = \rho v_s^2$ is reciprocal to the acoustic compliance from (2) and can be expressed as follows:

$$B_A = \frac{V}{C_A}. \tag{6}$$

Because the gas acts like a spring in the waveguide, the acoustic compliance is written as

$$C_A = \frac{1}{K_A} = \frac{S^2}{K}, \tag{7}$$

where K is the mechanical stiffness of the spring. Since the waveguide is the host frame of unit cell, the effective bulk modulus B_{eff} is defined as

$$B_{\text{eff}} = \frac{V}{C_{\text{eff}}}. \tag{8}$$

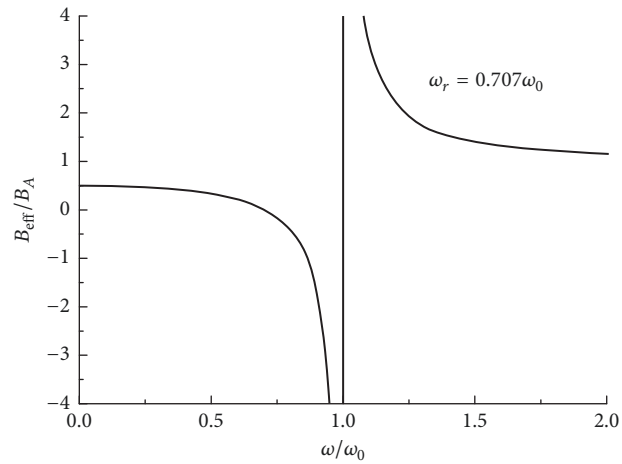

Figure 3: Effective bulk modulus of the unit cell obtained from the analytical expression.

Under the above assumption, acoustic impedance of the unit cell becomes

$$Z_a = j\omega L_A + \frac{1}{j\omega C_{\text{eff}}}. \tag{9}$$

Let us suppose that the waveguide has a larger cross section area and therefore the effective acoustic compliance C_{eff} is significantly greater than acoustic inertance L_A at near resonance frequency. Equation (9) is now

$$\begin{aligned} Z_a \approx \frac{1}{j\omega C_{\text{eff}}} &= \frac{(1/j\omega C_A)(j\omega L_r + 1/j\omega C_r)}{j\omega L_r + 1/j\omega C_A + 1/j\omega C_r} \\ &= \frac{1}{j\omega C_A}\frac{\omega^2 - \omega_r^2}{\omega^2 - \omega_0^2}, \end{aligned} \tag{10}$$

where $\omega_0^2 = \omega_A^2 + \omega_r^2$, $\omega_A = 1/\sqrt{L_r C_A}$, and $\omega_r = 1/\sqrt{L_r C_r}$. The effective acoustic compliance and effective bulk modulus are determined by the following expressions, respectively:

$$C_{\text{eff}} = C_A \frac{\omega^2 - \omega_0^2}{\omega^2 - \omega_r^2}, \tag{11}$$

$$B_{\text{eff}} = B_A \frac{\omega^2 - \omega_r^2}{\omega^2 - \omega_0^2}. \tag{12}$$

From (12), it can be seen that the inclusion of SHS in the waveguide results in the variation of effect bulk modulus of unit cell with frequency, as shown in Figure 3.

It can be seen that effective bulk modulus between frequencies $0 < \omega < \omega_r$ is greater than zero but is less than B_A. With the increasing of frequency, the effective bulk modulus is decreasing, because the acoustic inertance of SHS begins to take more effect. The frequency ω_r is the series resonance frequency of SHS unit. At this frequency, acoustic impedance is equal to zero which means the sound wave is by-passed and the effective bulk modulus is also zero.

In the frequencies range $\omega_r < \omega < \omega_0$, the inertia of SHS is so big that the effective bulk modulus is negative. The effective

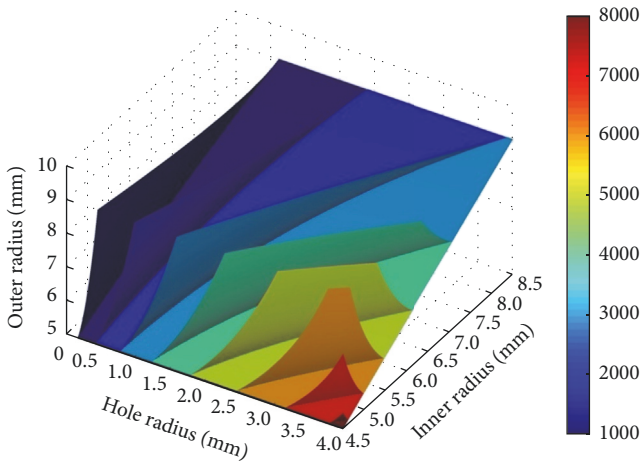

FIGURE 4: Relation between the parameters of SHS and the resonance frequency.

bulk modulus tends to minus infinity as frequency increases from ω_r to ω_0. It should be noted that the frequency ω_0 is the parallel resonance frequency of the ΔC_r and C_A and is also antiresonance frequency. At the frequency, the acoustic impedance is equal to minus infinity.

The effective bulk modulus is greater than zero in the frequency range above ω_0 and is greater than B_A. With the increasing of frequency, the effective bulk modulus is decreasing to B_A. It is also because of the more influence of the acoustic inertance of SHS.

2.3. The Resonance Frequency of SHS. From the above analysis, we can see that the resonance of SHS plays an important role in the negative effective bulk modulus of unit cell. Based on Helmholtz theory [21], the resonance frequency of SHS can be calculated by the similar LC circuit shown in Figure 1(a). The resonance frequency of SHS is

$$f_r = \frac{1}{2\pi\sqrt{L_r C_r}} = \frac{v_s}{2\pi}\sqrt{\frac{S_p}{L_p V_p}}. \tag{13}$$

The effective volume of cavity V_p, that is, the volume of inner sphere minus the volume of spherical crown as part of short-tube, is thus given by

$$\begin{aligned} V_p &= \frac{4}{3}\pi R_i^3 \\ &\quad - \pi\left(R_i - \sqrt{R_i^2 - a^2}\right)^2 \left(R_i - \frac{R_i - \sqrt{R_i^2 - a^2}}{3}\right), \end{aligned} \tag{14}$$

where $S_p = \pi a^2$ is the area of cross section of the short-tube.

The geometric length of the short-tube is

$$l_p = \sqrt{R_0^2 - a^2} - \sqrt{R_i^2 - a^2}. \tag{15}$$

Since the effective length of air in short-tube is longer than geometric length, we define it as the effective length L_p. In this model, the short-tube has two end corrections, where the outside of short-tube is considered as nonflange and the correction length is $0.61a$; the inside is under the flange state and the correction length is $(8/3\pi)a$ [22]. Thus, the effective length of short-tube is

$$L_p = \sqrt{R_0^2 - a^2} - \sqrt{R_i^2 - a^2} + 0.61a + \frac{8}{3\pi}a. \tag{16}$$

From the results given by (14) and (16), the amendment formula of resonance frequency is therefore

$$f_r = \frac{v_s}{2\pi}\sqrt{\frac{\pi a^2}{\left(\sqrt{R_0^2 - a^2} - \sqrt{R_i^2 - a^2} + 0.61a + (8/3\pi)\,a\right)\left[(4/3)\,\pi R_i^3 - \pi\left(R_i - \sqrt{R_i^2 - a^2}\right)^2\left(R_i - \left(R_i - \sqrt{R_i^2 - a^2}\right)/3\right)\right]}}. \tag{17}$$

In order to analyze the influence of geometrical parameters of SHS on tunable frequency, the relation between the three parameters of SHS and the resonance frequency was shown in Figure 4 based on formula (17). It can be seen that there is a lower resonance frequency as the neck size is smaller, and there is a higher frequency as the neck size is larger. This provides us an important way to precisely control acoustic metamaterial with negative effective modulus.

2.4. Simulation Results. The acoustic field is simulated by COMSOL Multiphysics 4.3 and the pressure acoustic and solid mechanics are coupled in the acoustic model for the continuity. The model consists of a SHS unit and a waveguide. The plane sound wave was used as a sound source and the other open end of outlet waveguide was modeled with PML boundary condition. The remaining boundaries of waveguide are specified as sound hard condition for the sound waves reflecting from waveguide wall completely. The material of wall of SHS is polyethylene and the fluid domain is full of air. At standard temperature and pressure conditions, the bulk modulus B_o of air is 1.42×10^5 Pa for an isentropic process. Suppose that $l = 20.0$ mm, $S = 225\,\pi\text{mm}^2$, $R_o = 5.0$ mm, $R_i = 4.5$ mm, and $a = 0.5$ mm to 2.5 mm (Figure 1(b)).

The results of the transmission spectrum are got and shown in Figure 5. Except that the curve of the radius of 0 mm has no transmission dip, there is a dip in every transmission curve. Furthermore, the blue shift of transmission dip occurs as the neck radius of SHS becomes bigger. According to (3),

Table 1: Relation between the neck radius and resonance frequency, (R_o = 5.0 mm, R_i = 4.5 mm).

The radius of neck/mm	0.5	1.0	1.5	2.0	2.5
Theoretical frequency/Hz	2200	3502	4602	5602	6491
Simulate frequency/Hz	2190	3514	4607	5594	6546

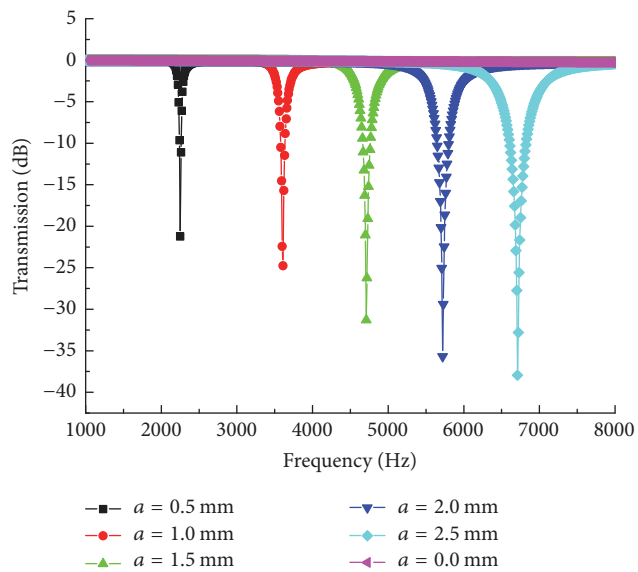

Figure 5: The transmission coefficients of Unit cell with different neck radius (R_o = 5.0 mm, R_i = 4.5 mm).

the increased quality of the air in the neck enhances its acoustic inertance, while the volume value of cavity has decreased slightly. In terms of the serial inductor-capacitor circuit, if the radius of cavity is constant, the inductance of the SHS decreases with increasing neck radius. Although the inner radius of SHS has not been changed, some volume of them becomes a part of the short-tube. The ability of storing energy of SHS gets weak and makes the capacitance of the resonator smaller. Hence, resonance frequency goes up with the increase of the neck radius of SHS.

The values of resonance frequency are shown in Table 1. For example, the SHS with 0.5 mm neck radius has phase reverse near the frequency of 2190 Hz for the local resonance. As is shown in Figure 6, the real part of effective modulus is negative near the resonance frequency of SHS, and it represents the character of the negative dynamic response. Similarly, effective modulus with different neck radius was obtained, and negative effective modulus near the resonance frequency is achieved individually (see Figure 6). This result is consistent with that described in [11].

For verifying the validity of formula (17), we calculate the values of resonance frequency with COMSOL method and amendment formula (17), and they were listed in Table 1. The simulated value of resonance frequency is in good agreement with the analysis results of the equivalent circuit. Thus, using formula (17), we can obtain the precise value and then control resonance frequency of SHS accurately.

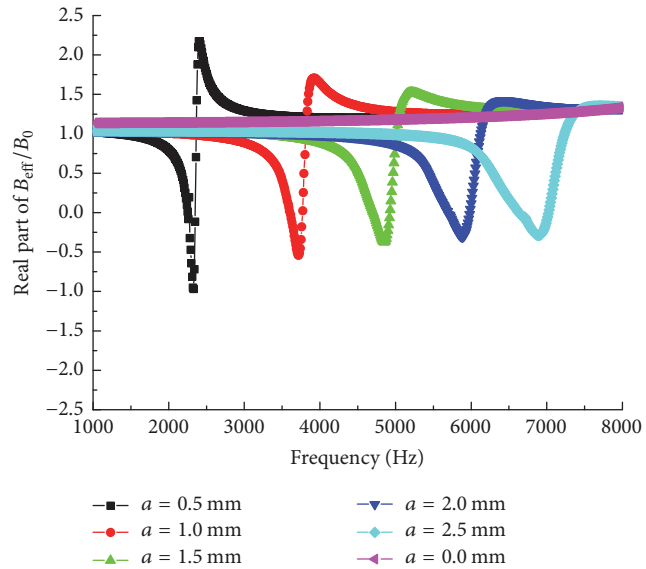

Figure 6: The effective modulus curves of unit cell with different neck radius (R_o = 5.0 mm, R_i = 4.5 mm).

3. Influence of Geometrical Parameters of SHS on Resonance Frequency

Similarly, the effects of other parameters on the tunable frequency of SHS were analyzed with COMSOL Multiphysics and formula (17) in the section. Formula (17) suggests that the tunable parameters of SHS include the hole radius, outer radius, inner radius of sphere cavity, and so on. Because the inner radius and neck radius affect the cavity volume, the difference between outer and inner radius acts as the length of short-tube, and the neck radius affects the area of cross section of short-tube. Thus, three characteristic parameters of SHS have a simultaneous influence on the tunable frequency. In this section, the effects of the inner and outer radius on the resonance frequency were mainly discussed.

3.1. The Inner Radius of SHS. Supposing that R_o = 9.0 mm, a = 0.5 mm, and R_i = 4.5 mm to 8.5 mm, the transmission spectrum are measured and shown in Figure 7. The resonance frequency decreases firstly and then increases with increasing the inner radius gradually. In addition, the negative modulus can be obtained near their respective resonance frequency. The results of formula calculation and the simulation agree well, which suggests that we can obtain the precise resonance frequency by formula (17) and accurately control the AM with SHS.

There is a V-type character of the resonant frequency and the minimum frequency value is at the inner radius with 7.5 mm. This phenomenon explained that the acoustic inductance of SHS decreases with increasing the inner radius; on the other hand, the acoustic capacitance increases with increasing the volume of cavity. Under the influence of two opposite aspect, the resonance frequency decreases firstly and then increases with the increase of the inner radius.

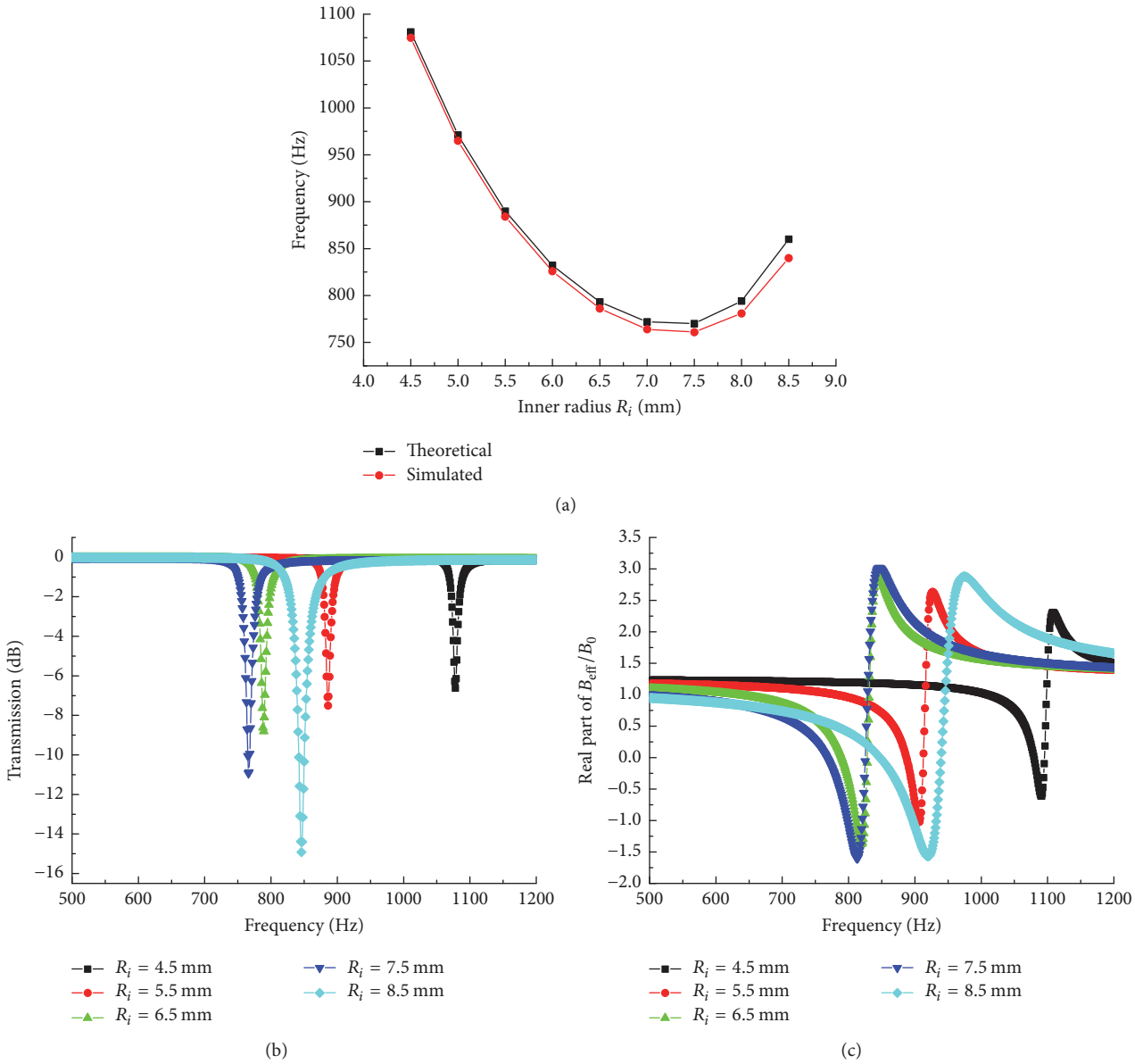

FIGURE 7: The relation curves present the relationship between the inner radius and related parameters (R_o = 9.0 mm, a = 0.5 mm). (a) The resonance frequency of SHS. (b) The transmission coefficient. (c) The effective modulus.

3.2. The Outer Radius of SHS. Supposing that R_i = 4.5 mm, a = 0.5 mm, and R_o = 5.0 mm to 9.0 mm, Figure 8 is the relation curves between the outer radius and related parameters, and the resonance frequency has a red shift with increasing the outer radius of SHS. This simulated result is in agreement with Helmholtz theory as well. In addition, the negative modulus can also be achieved near their respective resonance frequency.

The red shift explained that when the inner radius of SHS unchanged and the capacitance is constant, the sound energies of SHS unit with different outer radius are the same. However, the acoustic inductance of SHS increases with the increase of length of short-tube acted as inductor. Hence, the resonant frequency has a red shift.

The results of formula calculation and the simulation agree well, which suggests that we can obtain the precise resonance frequency by formula (17) and accurately control the acoustic metamaterial of SHS with negative modulus.

The results of formula calculation and the simulation agree well, which suggests that we can obtain the precise resonance frequency by formula (17).

4. Conclusion

Based on SHS unit, the tunable mechanism of structure size on controlling the resonance frequency of acoustic metamaterial with negative effective modulus was proposed from aspects of Helmholtz theory and the finite-element

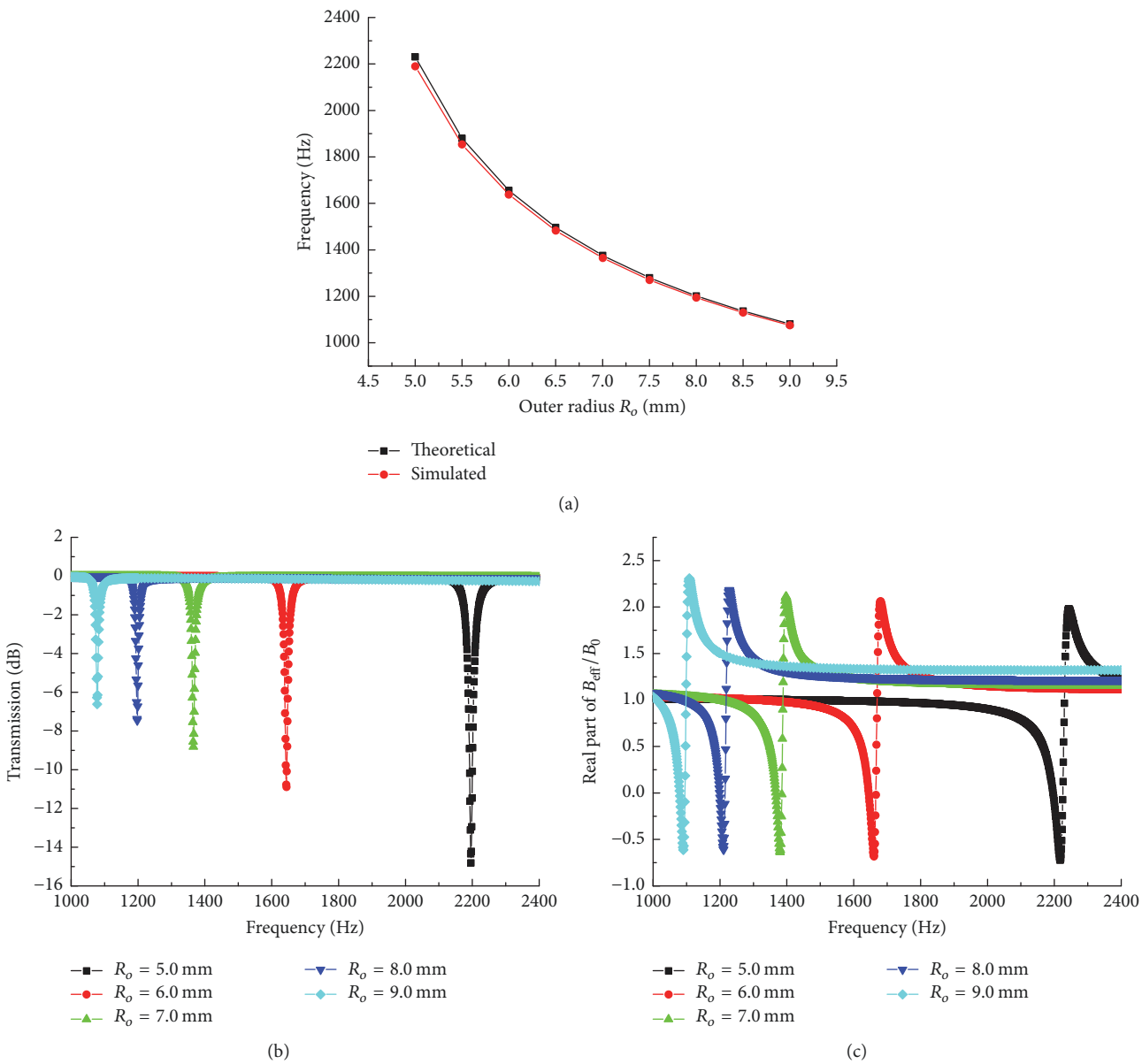

Figure 8: The relation curves present the relationship between the outer radius and related parameters (R_i = 4.5 mm, a = 0.5 mm). (a) The resonance frequency of SHS. (b) The transmission coefficient. (c) The effective modulus.

method. The amendment formula of resonance frequency of SHS was derived, and it can precisely describe the relation between resonance frequency and neck radius, inner radius and outer radius. Furthermore, COMSOL simulation was used to verify effectiveness of amendment formula, and it is revealed that simulated results of resonance frequency are in good agreement with theoretical results. The results indicate that the blue shift of resonance frequency occurs when the neck radius of SHS increases; the resonance frequency has a "V" change with the increase of inner radius of SHS; the resonance frequency has a red shift with increasing the outer radius of SHS. The method can precisely control the resonance frequency of acoustic metamaterial with negative effective modulus. There is a potential value on ultrasonic imaging, underwater acoustic, architectural acoustic, and sound absorbing material, and so on.

Conflicts of Interest

The authors declare that there are no conflicts of interest regarding the publication of this paper.

Acknowledgments

This work was supported by the National Natural Science Foundation of China (Grant nos. 11102164 and 11304243), the Natural Science Foundation of Shaanxi Province, China (Grant no. 2014JQ1039), the Scientific Research Program

Funded by Shaanxi Provincial Education Department (Grant no. 15JK1485), the Program of New Staff and Research Area Project of NPU (Grant no. 13GH014602), and the Cultivation Fund of Xi'an University of Science and Technology (Grant no. 2009029).

References

[1] Z. Liu, X. Zhang, Y. Mao et al., "Locally resonant sonic materials," *Science*, vol. 289, no. 5485, pp. 1734–1736, 2000.

[2] Z. Yang, J. Mei, M. Yang, N. H. Chan, and P. Sheng, "Membrane-type acoustic metamaterial with negative dynamic mass," *Physical Review Letters*, vol. 101, no. 20, Article ID 204301, 2008.

[3] C.-L. Ding and X.-P. Zhao, "Audible sound metamaterial," *Acta Physica Sinica*, vol. 58, no. 9, pp. 6351–6355, 2009.

[4] J. Pierre, B. Dollet, and V. Leroy, "Resonant acoustic propagation and negative density in liquid foams," *Physical Review Letters*, vol. 112, no. 14, Article ID 148307, 2014.

[5] M. Yang, G. Ma, Z. Yang, and P. Sheng, "Coupled membranes with doubly negative mass density and bulk modulus," *Physical Review Letters*, vol. 110, no. 13, Article ID 134301, 2013.

[6] J. J. Park, C. M. Park, K. J. B. Lee, and S. H. Lee, "Acoustic superlens using membrane-based metamaterials," *Applied Physics Letters*, vol. 106, no. 5, Article ID 051901, 2015.

[7] K. Song, S.-H. Lee, K. Kim, S. Hur, and J. Kim, "Emission enhancement of sound emitters using an acoustic metamaterial cavity," *Scientific Reports*, vol. 4, article no. 4165, 2014.

[8] J. Liu, Z. L. Hou, and X. J. Fu, "Mechanism for local resonant acoustic metamaterial," *Acta Physica Sinica*, vol. 64, no. 15, Article ID 154302, pp. 54302–154302, 2015.

[9] X. W. Yang, J. S. Lee, and Y. Y. Kim, "Effective mass density based topology optimization of locally resonant acoustic metamaterials for bandgap maximization," *Journal of Sound and Vibration*, vol. 383, no. 11, pp. 89–107, 2016.

[10] A. O. Krushynska, V. G. Kouznetsova, and M. G. Geers, "Visco-elastic effects on wave dispersion in three-phase acoustic metamaterials," *Journal of the Mechanics and Physics of Solids*, vol. 96, no. 11, pp. 29–47, 2014.

[11] N. Fang, D. Xi, J. Xu et al., "Ultrasonic metamaterials with negative modulus," *Nature Materials*, vol. 5, no. 6, pp. 452–456, 2006.

[12] S. H. Lee, C. M. Park, Y. M. Seo, Z. G. Wang, and C. K. Kim, "Acoustic metamaterial with negative modulus," *Journal of Physics: Condensed Matter*, vol. 21, no. 17, Article ID 175704, 2009.

[13] C. Ding, L. Hao, and X. Zhao, "Two-dimensional acoustic metamaterial with negative modulus," *Journal of Applied Physics*, vol. 108, no. 7, Article ID 074911, 2010.

[14] X. Jing, Y. Meng, and X. Sun, "Soft resonator of omnidirectional resonance for acoustic metamaterials with a negative bulk modulus," *Scientific Reports*, vol. 5, no. 11, Article ID 16110, 2015.

[15] W. Akl and A. Baz, "Multi-cell active acoustic metamaterial with programmable bulk modulus," *Journal of Intelligent Material Systems and Structures*, vol. 21, no. 3, pp. 541–556, 2010.

[16] X. Yu, Z. Lu, F. Cui, L. Cheng, and Y. Cui, "Tunable acoustic metamaterial with an array of resonators actuated by dielectric elastomer," *Extreme Mechanics Letters*, vol. 12, pp. 37–40, 2017.

[17] B. Xia, N. Chen, L. Xie, Y. Qin, and D. Yu, "Temperature-controlled tunable acoustic metamaterial with active band gap and negative bulk modulus," *Applied Acoustics*, vol. 112, no. 11, pp. 1–9, 2016.

[18] C. L. Ding, X. P. Zhao, L. M. Hao, and W. R. Zhu, "Acoustic metamaterial with split hollow spheres," *Acta Physica Sinica*, vol. 60, no. 4, Article ID 044301, 2011.

[19] L.-M. Hao, C.-L. Ding, and X.-P. Zhao, "Tunable acoustic metamaterial with negative modulus," *Applied Physics A: Materials Science & Processing*, vol. 106, no. 4, pp. 807–811, 2012.

[20] L.-M. Hao, C.-L. Ding, and X.-P. Zhao, "Design of a passive controllable negative modulus metamaterial with a split hollow sphere of multiple holes," *Journal of Vibration and Acoustics*, vol. 135, no. 4, Article ID 041008, 2013.

[21] G. H. Du, *Fundamentals of Acoustics*, Nanjing University Press, Nanjing, China, 2012.

[22] D. T. Blackstock, *Fundamentals of Physical Acoustics*, John Wiley & Sons, NJ, USA, 2000.